Application of UV-Vis-NIR Spectroscopy to Gemology

Shiyun Jin, Nathan D. Renfro, Aaron C. Palke, Troy Ardon, and Artitaya Homkrajae

Optical spectroscopy, also known as ultraviolet/visible/near-infrared spectroscopy, measures how electromagnetic radiation around the visible range is preferentially absorbed by a gemstone. A transparent gemstone can absorb certain wavelengths of light that pass through it, creating color in the transmitted light, whereas an opaque gemstone absorbs light on its surface and creates color in the reflected light. The physics of how electromagnetic radiation of different wavelengths interacts with materials is summarized to provide a basic understanding of how electronic transitions in gemstones can cause different colors. The different instruments and configurations suitable for various gemstone types are also explained. Specific routine applications of ultraviolet/visible/near-infrared spectroscopy to colored gemstones, fancy-color diamonds, and saltwater pearls are summarized, showcasing how identifying the chromophores in gemstones can facilitate varietal calls, origin determination, and treatment detection in a gemological laboratory.

The color of a colored gemstone, fancy-color diamond, or pearl is one of the most important aspects determining its desirability and value. Colors can be induced by trace elements, structural defects, or even organic pigments in gemstones, which may be removed, altered, or enhanced through various treatment processes. Even though the average human eye can differentiate millions of colors, the color space is limited to three dimensions, as our eyes only have three different types of cone cells, which are sensitive to different wavelengths of light. Therefore, very similar colors in our vision may be created by completely different chromophores in a gemstone. Moreover, our eyes cannot detect any light beyond the visible range. Therefore, optical spectroscopy in the visible (Vis) spectrum range, along with the adjacent ultraviolet (UV) and near-infrared (NIR), is one of the most important analytical testing techniques in gemology. UV-Vis-NIR spectroscopy, commonly referred to as UV-Vis, measures how light is attenuated by absorption inside or on the surface of a transparent or opaque gemstone, respectively. The details in the absorption spectrum can provide information about the trace element chemistry, defect configurations, and organic pigments that may help identify a gem's species, variety, and potential treatments.

In 1666, Sir Isaac Newton used a glass prism to explore the phenomenon of color in sunlight (Anderson and Payne, 1998), which opened an entirely new physics field of optics. Centuries later, gemologists would regularly use the same principles described by Newton to unravel the origin of color in gemstones. Gemologists have applied spectroscopy to gemstones since the 1930s (Anderson and Payne, 1998). In general, they used handheld spectroscopes to split light into its component colors and observe with their eyes the light not absorbed by the gemstone as bright spectral colors, in contrast to dark bands or sharp black lines representing the areas in the visible spectrum where the gem did absorb light. Many of these

In Brief

- UV-Vis-NIR spectroscopy can resolve the details in the absorption spectrum of gem materials that cannot be detected by the eye.
- Absorption of ultraviolet, visible, and near-infrared radiation is caused mainly by electronic transitions in the outer shells around the atoms in a material.
- UV-Vis-NIR spectroscopy is a quick routine analysis with a wide range of applications in testing colored stones, fancy-color diamonds, and pearls.

See end of article for About the Authors and Acknowledgments.
Gems & Gemology, Vol. 60, No. 4, pp. 456–473,
http://dx.doi.org/10.5741/GEMS.60.4.456

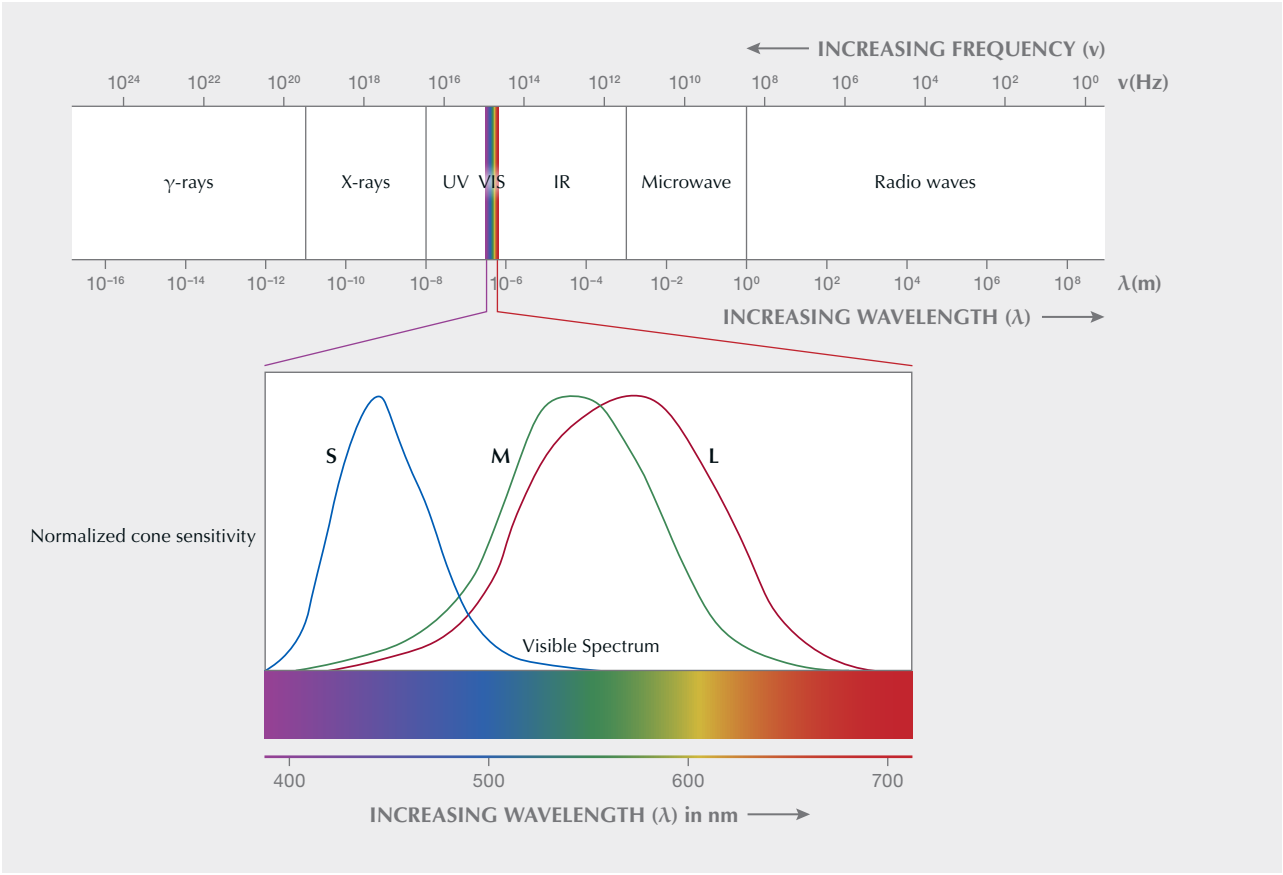

Figure 1. Schematic diagram showing the relation between the visible spectrum and the entire electromagnetic spectrum. The normalized sensitivity curves of three types of cone cells (L: long, M: medium, and S: short) in the human eye are plotted over the visible spectrum.

early observations were documented in articles by Basil Anderson in *The Gemmologist* (see also Anderson et al., 1998). Other references on spectroscopy also became available, such as the 114 spectra recorded by Robert Crowningshield for the 1962 edition of Richard T. Liddicoat's *Handbook of Gem Identification* (Moses and Shigley, 2003). *Gems & Gemology*'s Lab Notes section also became a regular forum for new spectroscopic observations by Crowningshield, who was a pioneer in the field.

In the late 1980s, optical engineers with GIA Gem Instruments developed a digital scanning diffraction grating spectroscope called the DISCAN, which allowed users to precisely measure the position of absorption features (Koivula and Kammerling, 1989). In the early 2000s, advancements in technology led to the development of spectrometers that significantly reduced the measurement time required to collect UV-Vis-NIR spectra, while also making the instruments much more compact and portable (Breeding et al., 2010). While the handheld spectroscope is still widely used in gemology courses, spectrometers have become widely available. In the future, we may see the handheld spectroscope essentially replaced with even smaller compact spectrometers that can quickly measure and record data on gemstones.

THE ELECTROMAGNETIC SPECTRUM AND ITS INTERACTION WITH MATERIALS

Just as ripples spread across the surface of water that has been disturbed, a disturbance in the electromagnetic field can propagate through space as electromagnetic radiation, or an electromagnetic wave. The wavelengths of electromagnetic waves range from ~10^{-15} m to ~10^{5} m. Due to their dramatically different properties, the electromagnetic spectrum is broadly classified into different categories with de-

creasing wavelengths (figure 1): radio waves, microwaves, infrared (IR), visible light, ultraviolet, X-rays, and gamma rays. However, because the electromagnetic spectrum is continuous, the boundaries between two adjacent categories are generally blurred and can vary depending on specific applications. The exception is visible light, which has a well-defined range of 400 to 700 nm (again, see figure 1). The boundary between what a human eye can and cannot see is relatively sharp, although the exact range varies slightly from one individual to another.

The energy of an electromagnetic wave is proportional to its frequency (f) and inversely proportional to its wavelength (λ). This means that shorter wavelengths correspond to higher-energy electromagnetic waves. Because this inverse relation between wavelength and energy is sometimes inconvenient, the quantity wavenumber ($\tilde{\nu}$, in units of cm^{-1}), which is the inverse of wavelength, is often used in spectroscopy, though more commonly for Fourier-transform infrared (FTIR) and Raman spectroscopy (see Breeding and Ahline, 2024, pp. 474–492 of this issue; Jin and Smith, 2024, pp. 518–535 of this issue). The wavelength (in nm) and wavenumber of an electromagnetic wave can be converted between one another using the following equation:

$$\tilde{\nu}\ (cm^{-1}) = \frac{10000000}{\lambda\ (nm)} \quad (1)$$

An electric field exerts a force on a charged particle, causing it to accelerate. An electromagnetic wave, which consists of alternating electric and magnetic fields, makes a charged particle oscillate by moving it back and forth, transferring the energy from the radiation to the charged particle. This is the basic principle of how electromagnetic radiation interacts with materials. All materials in everyday life are composed of charged particles such as electrons and protons, which can be accelerated by electromagnetic radiation. The energy transfer between electromagnetic radiation and a material is most efficient when the wave frequency resonates with the intrinsic frequency of a specific transition in the material—that is, when the energy of the electromagnetic radiation matches the energy difference between two states in the material. For instance, microwaves can excite the low-frequency movements of polar molecules (e.g., water molecules) and thus can be used to heat food. IR radiation has energies similar to vibrations of individual covalent bonds (e.g., OH bonds in water and other hydrous materials) or vibrations of the entire crystal lattice (Breeding and Ahline, 2024); X-rays can excite the high energy electrons in the innermost orbitals of an atom, which is why X-ray fluorescence can be used to analyze the chemical composition of a material (Sun et al., 2024). The most energetic gamma rays, which come from nuclear reactions, are the only photons that can excite the nuclei of atoms.

With energies falling in between X-rays and IR, ultraviolet and visible light mostly interact with the valence and outer-shell electrons of a material. These electronic transitions are very complex quantum mechanical processes that can be described by several different theories, depending on the system (e.g., ligand field theory, molecular orbital theory, crystal field theory, and band theory) (Rossman, 2014). Generally, the electrons in the outer shells of an ion in a material can be excited in several different ways. They may be elevated to a higher energy state around the same ion (i.e., electronic transitions in the transition metals or rare earth elements). They may transfer to orbiting a different ion, such as the charge transfer between an anion and a cation, or the intervalence charge transfer (IVCT) between two cations with variable oxidation states. In a semiconductive material, electrons can be excited all the way up to the conduction band. Electrons in a material can sometimes be displaced and trapped, typically by ionizing radiation (alpha, beta, and gamma rays), which creates electron-hole centers that can be excited by photons in the UV-Vis range.

Various colors are created when certain sections of the visible spectrum are preferentially absorbed by specific electronic transitions. The human eye has only three types of cone cells, each sensitive to a different region of the visible spectrum: red (long wavelength), green (medium wavelength), and blue (short wavelength) (again see figure 1). Color is perceived based on the relative intensities of these three light regions as they excite each type of cone cell in our vision. This is the basis of the RGB color system. Due to the limited number of cone types, different spectral compositions may appear as the same color to our eyes if they excite the same reactions of the cone cells. That is why we need the entire visible absorption spectrum to reveal the color-causing trace element or defect in a gemstone. Although only the absorption features within the visible spectrum can affect the color or appearance of a gemstone, the underlying physical processes could extend beyond the visible spectrum into the UV or IR range. Therefore, optical absorption spectroscopy is not limited only to visible light but includes the ultraviolet and near-infrared as

well, collectively known as UV-Vis-NIR spectroscopy. This is one of the main advantages of an electronic spectrometer over a handheld spectroscope, which only reveals absorption features in the visible range due to the limitations of the human eye.

Note that the light-absorbing electronic transitions are dependent on the valence states or configurations of the trace elements and defects, which are often determined by oxidation conditions or radiation damages. Thus, these transitions can be enhanced, modified, or removed through heat or radiation treatments or by introducing additional chemical components through diffusion (Emmett and Douthit, 1993; Kitawaki et al., 2006; Jollands et al., 2023). These processes may occur either naturally in geological processes or artificially in a gem treatment facility. While UV-Vis-NIR spectroscopy is seldom diagnostic for specific gemstone treatments, it can often help narrow down the number of potential treatments or eliminate the possibility of treatment altogether, expediting testing in a gemological laboratory by removing unnecessary steps.

Adding another layer of complexity, visible light also interacts with nanoscale textures in a material that can create optical and color effects. Conductive nanoparticles can preferentially absorb visible light of certain wavelengths due to the surface plasmon (a quantized collective vibration of electron clouds) on the interface between the particle and the matrix. For instance, the red and green colors of Oregon sunstone are caused by copper nanoparticle inclusions <50 nm (Jin et al., 2022, 2023). Nanoparticles can also preferentially scatter light of specific wavelengths—known as Rayleigh scattering, Mie scattering, or Tyndall scattering depending on the size, shape, or dielectric properties of the particles—which can create opposite colors in transmission and scattered light (Jin et al., 2023). Periodic nanotextures in labradorite, precious opal, or agate can cause an interference effect known as diffraction, which produces iridescent colors that sometimes change with viewing angle (Baier, 1932; Bolton et al., 1966; Heaney, 2021). The color effects created by special nanostructures are known as "structural colors," which are sometimes considered "not real" in comparison to the pigment colors created by electronic transitions and thus sometimes referred to as "pseudochromatic" colors. Except for special research purposes, the structural colors are typically not of interest for UV-Vis-NIR analyses in a gemological laboratory and mostly pose an inconvenience for data collection and interpretation.

The oscillating electric (and magnetic) field in a beam of light can be directional, which is known as its polarization. Similarly, the electronic transitions or nanoscale textures in a material can also be directional, absorbing or scattering photons of different polarization with different efficiencies. Therefore, the optical spectrum may depend on the sample's orientation relative to the polarization of the light source. Optically isotropic (singly refractive) gemstones such as diamond, spinel, garnet, or strain-free glass are not affected by this phenomenon; it is only observed in optically anisotropic (doubly refractive) gemstones, which often display pleochroism and show different colors under the dichroscope. The optical properties of doubly refractive materials such as feldspar, tourmaline, and corundum can be extremely complicated (Dowty, 1978; Dubinsky et al., 2020; Jin et al., 2023) and are beyond the scope of this article. Polarized light is rarely used for qualitative analysis on doubly refractive gems in a gemological laboratory, though multiple measurements along different directions may be performed on intensely pleochroic samples to account for anisotropy.

PRACTICAL APPLICATIONS TO GEMOLOGY

The distinct spectra of colored gemstones, fancy-color diamonds, and pearls can be a powerful tool for identification, origin determination, and treatment detection. The technical details of how UV-Vis-NIR spectra are measured and quantified in a gemological laboratory are described in boxes A and B. As new discoveries about the absorption properties of gemstones emerge, our understanding of gemology continues to evolve. While the applications of UV-Vis-NIR spectroscopy in this field are far too numerous to detail in this article, those most routinely used in GIA laboratories are summarized here.

Colored Stones. Most applications of UV-Vis-NIR spectroscopy for colored stones focus on the identification of specific chromophores. For certain types of gems, the variety can be determined based on specific color-causing agents. The presence or absence of certain spectroscopic features beyond the visible range, in the UV or NIR regions, further assists in identification, making the spectrometer a much more useful tool than a handheld spectroscope.

Copper-Bearing Blue-Green Tourmaline. One of the most common applications of UV-Vis-NIR spectroscopy is the separation between tourmaline

BOX A: ABSORPTION OF LIGHT: MEASUREMENT AND QUANTIFICATION

A light detector, such as a photomultiplier tube or charge-coupled device (CCD) sensor, measures the intensity of light attenuated by the material at each wavelength and compares it to the unattenuated intensity of the light source. The attenuation measured may come from absorption, surface reflection, internal reflection, or scattering from inclusions and other internal textures. These factors can complicate the data interpretation. The simplest way to measure the attenuation spectrum of a transparent material is to use a direct light path. In this approach, the unblocked intensity of the light source is measured as the background, and the attenuated intensity is measured by passing light through the sample (figure A-1A). Transmittance (T) is the fraction of the incident light power that is transmitted through the sample (often expressed as a percentage). It is simply the ratio of the attenuated intensity (I_T) to the unattenuated intensity (I_0) measured by the detector:

$$T = \frac{I_T}{I_0} \quad \text{(A-1)}$$

Absorbance (A) is defined as the negative logarithm of transmittance:

$$A = -\log T = \log \frac{I_0}{I_T} \quad \text{(A-2)}$$

Assuming the contributions from surface reflection and internal scattering are negligible, the absorbance is proportional to the length of the light path in the material (l) and the concentration of the attenuating species (c), such as light-absorbing elements or defects. This linear relationship is known as the Beer-Lambert law:

$$A = \varepsilon l c \quad \text{(A-3)}$$

where ε is the molar absorption coefficient of the absorbing species. In theory, this law can be used to quantify the absolute concentration of certain chromophores in a gemstone (Dubinsky et al., 2020), though in practice it is very difficult due to the irregular shapes, optical anisotropy, and heterogeneity of most gem materials. Except for the special case of copper-colored feldspars (or copper- or gold-colored glass), all the known absorption

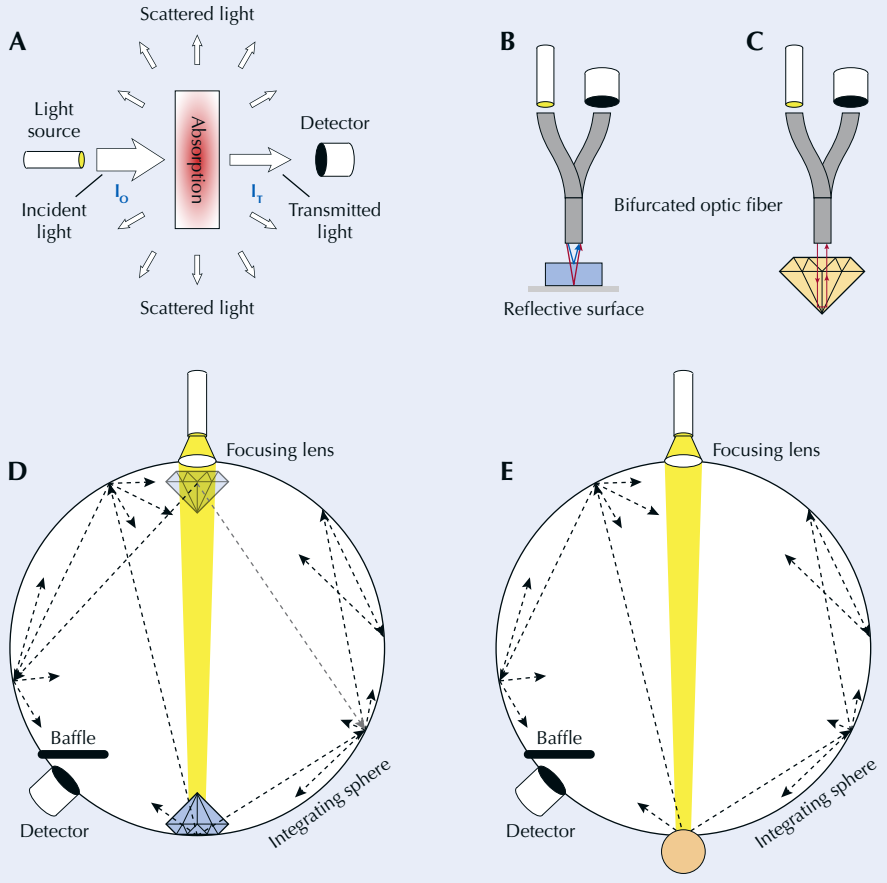

Figure A-1. A: The simplest configuration for measuring transmittance and absorbance with a direct light path through a wafer-shaped sample. B: A reflective configuration with a bifurcated optical fiber, which can be used to measure the surface reflectance of an opaque material (blue path) and transmittance through a wafer placed on a reflective surface (red path). C: Transmittance through a faceted stone can be measured using the internal reflection created by its pavilion facets. D: A common configuration for measuring the absorption of an irregularly shaped transparent sample, which can be placed anywhere inside the integrating sphere as long as it completely covers the incident light. E: A similar configuration as in C, but for measuring the reflectance of opaque samples with irregular or unsmooth surfaces (e.g., pearls) placed outside the sphere.

features (i.e., nonstructural colors) in gemstones are caused by transitions involving valence or outer-shell electrons.

For opaque materials such as pearls that do not transmit light, transmittance or absorbance cannot be measured. Unlike transparent materials, where color is determined by the transmitted light, the light reflected off the surface determines the color and appearance of an opaque material. Rather than the intensity of transmitted light, the intensity of reflected light should be measured for opaque materials. Reflectance (R) is defined as the proportion of incident power that is reflected by the surface:

$$R = \frac{I_R}{I_0} \quad \text{(A-4)}$$

For a well-polished surface that allows specular reflection, reflectance can be measured simply by shining the incident light perpendicular to the surface and collecting the light reflected directly back (figure A-1B, blue path). Due to the different configuration of the spectrometer, the incident intensity I_0 for reflectance cannot be directly measured the same way as for transmittance. A special reflective material that evenly reflects more than 99% of the light back to the detector is needed to acquire the reference background.

Note that the luster of a transparent gemstone comes mainly from its surface reflectance, which is mostly independent of wavelength. Therefore, it is meaningless to measure the surface reflection spectrum of a transparent gemstone. However, if a transparent wafer is placed on top of a reflective surface (figure A-1B, red path), the reflected light measured by the detector will have passed through the wafer twice (before and after reflecting). This allows transmittance and absorbance to be measured using the reflection configuration. In fact, the reflective surface is not even needed for a faceted transparent gemstone cut to maximize light return, because the incident light will reflect back to the detector off the pavilion facets (figure A-1C). This type of measurement is routinely used in gemological laboratories and is particularly useful for mounted stones, through which direct transmittance is impossible to measure.

Accurate quantification of the absorptivity of a specific chromophore in a host material requires creating a wafer-shaped sample with two parallel polished surfaces to ensure a straight light path (with a consistent path length) through the sample (figure A-1A). For anisotropic materials, polarized light aligned with the optical orientation of the analyzed material is also necessary. Such quantitative analysis is obviously infeasible for gemological testing, as it would require destructive reshaping of the material. But due to the linear nature of absorbance, only qualitative analyses are needed for gemological testing, because the overall shape of the absorption spectrum of a gemstone is independent of its size or cut, depending only on the absorptivity ε and relative concentrations of chromophores (if multiple chromophores are involved). Transmittance, on the other hand, is not a linear quantity, so the transmission spectrum will change shape depending on the absolute values of the light path length and chromophore concentrations. As a result, the appearance of a gemstone—its hue, tone, and color saturation, as determined by light transmitted through the stone—may depend considerably on its size and cut. Therefore, the transmission spectrum is needed to calculate the color of a transparent gemstone. Similarly, the reflectance or backscattered spectra are used to calculate the color of an opaque or translucent gemstone.

The facets or curved surfaces of cut stones can refract and reflect light unpredictably, preventing the accurate measurement of transmittance, absorbance, or reflectance. Most gemstones are neither perfectly transparent nor completely opaque but lie somewhere in between. Almost all transparent gemstones contain some inclusions that could distort the measurement of absorption by scattering light away from a straight path. Translucent and semitransparent materials allow some light to transmit through but also scatter or reflect a significant portion of light back. The light transmitted through such materials might be too weak to measure using transmission spectroscopy. Although it may be possible to measure backscattered light using reflection spectroscopy, this technique often lacks the features gemologists need to identify a stone.

To reduce the undesired and unpredictable effects of internal scattering and surface reflections, a special optical device known as an integrating sphere is often used in a UV-Vis-NIR spectrometer (figure A-1, D and E). An integrating sphere is simply a spherical cavity with a diffusively reflective coating on the inside, with a few ports for incident light, detector, and sample placement. Light entering the integrating sphere bounces around randomly multiple times due to the reflective surface before exiting through the detector port, blending the transmitted, scattered, and reflected light together and allowing only the contribution from absorption to be measured. Transparent gemstones must be placed inside the integrating sphere (figure A-1D) to prevent light from leaking out, whereas opaque samples such as pearls can be placed outside the sphere as long as they cover the sample port (figure A-1E). The exact position of the sample inside the integrating sphere does not matter, as long as all incident light is attenuated by the sample before being integrated by the sphere. A lens is often used to focus the incident light through the sample on the opposite side of the integrating sphere so that absorbance and reflectance can be measured using the same configuration (figure A-1, D and E). Positioning the sample on the opposite side of the light source also allows it to be placed on a metal stage cooled by liquid nitrogen, which is often used for testing diamonds.

Box B: Optical Spectrometers

The equations and measurement configurations explained in box A (figure A-1) consider light as a single entity. However, absorption (or reflection) spectroscopy requires the measuring of absorbance (or reflectance) at each individual wavelength, and this involves splitting light into different wavelengths. There are two physical processes for splitting polychromatic light (light containing multiple colors) into a spectrum of different wavelengths: dispersion and diffraction. The refractive index of a transparent material is often dependent on wavelength, which means light of different wavelengths may be refracted at different angles, allowing light to be dispersed into its spectral components by a prism. (This was how Sir Isaac Newton discovered that white light consists of a mixture of different colors.) Diffraction, on the other hand, takes advantage of how light interferes differently depending on wavelengths and scattering angles. A diffraction grating is an optical device that uses diffraction to split light (Jin and Smith, 2024). Both dispersive prisms and diffraction gratings can be used to make spectroscopes, while diffraction gratings are much more commonly used in spectrometers due to their higher efficiency and accuracy.

A scanning spectrophotometer scans through the spectrum range and measures the light intensity at each wavelength one at a time (figure B-1, top). After the white light source is separated into different wavelengths, only a very narrow range of wavelengths is allowed to pass through a narrow exit slit to the sample and be measured by the detector. The wavelength of light that passes through can be accurately controlled by adjusting the relative angle between the diffraction grating (or optical prism) and the exit slit (the actual optics are much more complicated than shown in figure B-1). This optical device that reduces polychromatic light (consisting of multiple wavelengths) to monochromatic light (of a single wavelength) is called a monochromator. The box with a dashed outline in figure B-1 (top) is a common example. The complete optical spectrum is measured by scanning the monochromator across the desired range. An optional second monochromator tuned to the same wavelength as the incident light can be positioned after the sample and before the detector to filter out any luminescence from the sample, allowing only attenuated light of the same wavelength to pass through to the detector.

In a CCD spectrometer, white light passes directly through the sample before being separated into its spectral components by a stationary dispersion device (figure B-1, bottom). An elongated CCD detector covering the

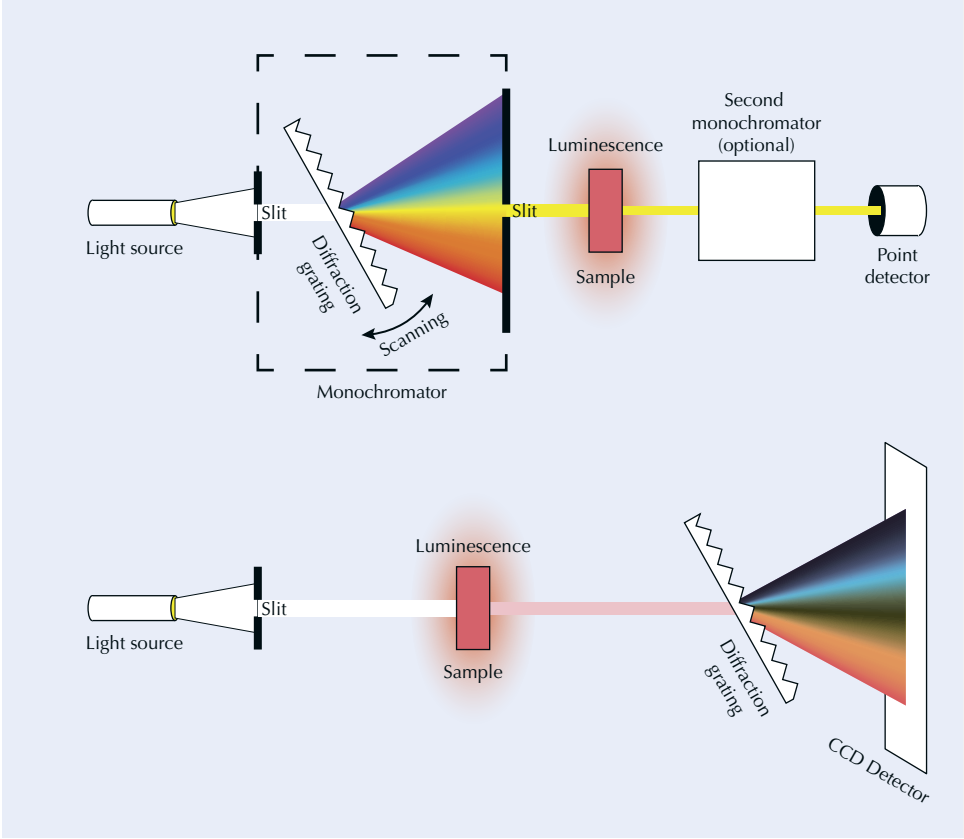

Figure B-1. Schematic comparison of the scanning spectrophotometer (top) and the CCD spectrometer (bottom). The scanning spectrophotometer measures absorbance at each wavelength sequentially, whereas the CCD measures the entire spectrum simultaneously. The CCD detector cannot remove luminescence from the sample excited by the incident light, which may affect the shape of the measured spectrum. Transmission gratings are shown for simplicity, though in reality, reflective gratings are more common in monochromators and CCD spectrometers.

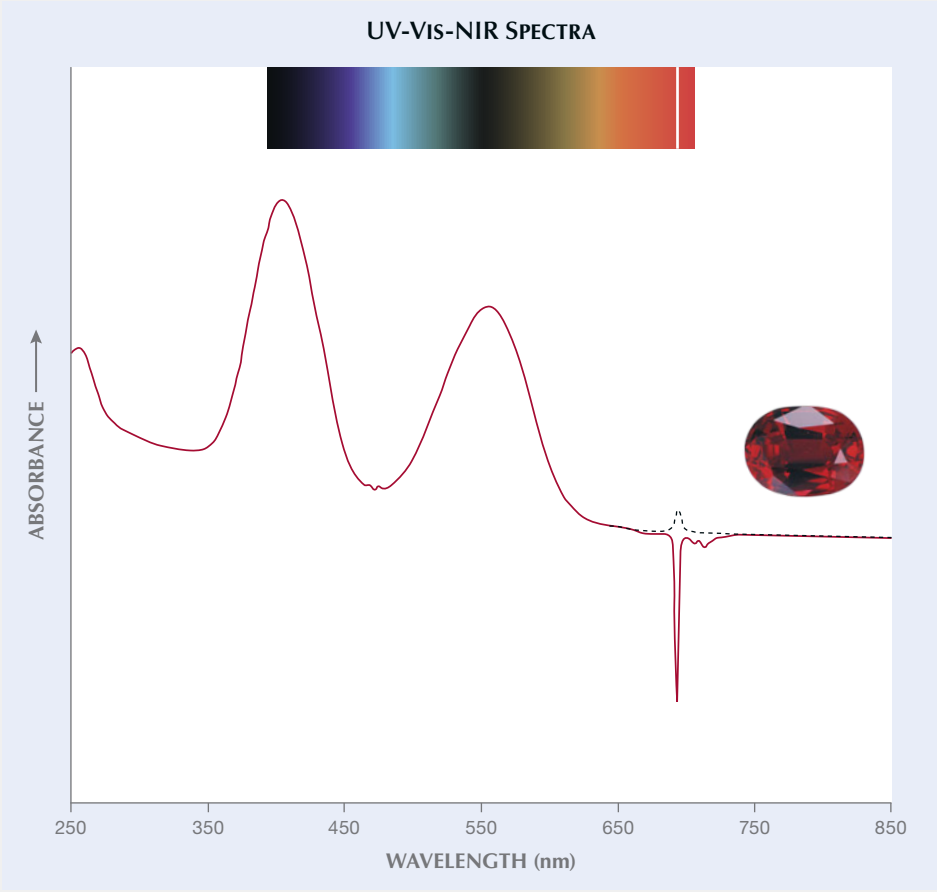

Figure B-2. The absorption spectrum of a synthetic ruby measured using a CCD spectrometer is compared to the view in a spectroscope. Absorption peaks in the spectrum appear as dark bands in the spectroscope. The CCD spectrometer has a much wider range than the spectroscope. A scanning spectrophotometer can have an even wider range, extending from 200 to 2500 nm. The sharp Cr^{3+} fluorescence peak at 694 nm appears as a negative dip, as the "attenuated" light intensity at this wavelength is stronger than the unattenuated incident light. Similarly, a sharp, bright line may be observed in the spectroscope. This type of artifact can be easily recognized for sharp luminescence features but may be overlooked if the luminescence band is broad. A scanning spectrophotometer avoids this artifact by measuring one wavelength at a time, revealing a sharp absorption peak at 694 nm (black dashed line).

entire angle of the dispersed spectrum is positioned at the end. By using well-characterized emission features of known materials, the detector can be calibrated to accurately correlate each pixel on the CCD to a specific wavelength. Note that a handheld spectroscope is essentially a simplified version of a CCD spectrometer, with a human eye in place of the CCD detector. Of course, the human eye can only detect light within the visible spectrum and will miss any features in the UV or NIR range.

The relationship between scanning and CCD spectrometers is analogous to that between the two types of X-ray diffractometers (Jin and Smith, 2024). The scanning spectrophotometer is much more accurate in measuring intensity at each specific wavelength and removes any potential interference from sample luminescence. Light polarizers can be implemented to allow measurement of polarized spectra. However, the geometry of the monochromators before and after the sample significantly limits the flexibility of this device, making it suitable almost exclusively for measuring transparent wafers in a direct light path (figure A-1A). The high-precision optics in the monochromators in scanning spectrophotometers also make them very expensive, limiting their availability to research or industrial facilities. Scanning through a desired range of the spectrum can be time-consuming, especially when high spectral resolution and high accuracy are needed.

The more affordable CCD spectrometers offer a number of advantages. They can make measurements much more rapidly because they capture the entire spectral range simultaneously, and the signal reaching the detector can be integrated repeatedly over a period of time to improve the signal-to-noise ratio. And because unseparated white light is used through most of the optics until the final part before the CCD detector (figure B-1, bottom), the configuration is much more flexible, allowing measurement of opaque and irregularly shaped samples, especially while using integrating spheres (figure A-1, B–E). As a result, CCD spectrometers have become much more widely used for gemological applications. However, one significant disadvantage is that these spectrometers cannot correct for photoluminescence excited by the incident light from the sample (figure B-1, bottom). Sharp-band luminescence features are easily identifiable (e.g., the Cr^{3+} band in ruby, as shown in figure B-2), whereas broad emission

bands can potentially alter the shape of the absorption spectrum in a way that is not noticeable.

It should be noted that the detector in a spectrometer can only measure light intensities within a certain range. Below this range, any signal is indistinguishable from noise. Above it, the detector is saturated and every signal is registered as the same value. The ratio of the maximum value to the minimum value a detector can measure is known as its dynamic range. For a detector with a dynamic range of 1000:1, if the unattenuated intensity of the light source is barely saturating the detector, the lowest transmittance the detector could measure would be 1/1000 (or 0.1%), meaning the largest absorbance that can be measured is 3 (i.e., $\log_{10}1000$). Both the light source intensity and the dynamic range of the detector are wavelength-dependent, which means the measurable range for absorbance by a spectrometer is limited by its weakest point in the spectrum. Most spectrometer software plots unmeasurable absorbance as a constant value above the highest value that can be theoretically measured to avoid confusion, sometimes causing the absorption spectrum to appear as a perfectly flat line when it reaches a certain value. It may be possible to extend the dynamic range by attenuating the light source with a filter of known absorbance or breaking the spectrum into several parts that can be optimized separately. Reducing the light path length (e.g., measuring along a shorter dimension or the edge of the sample) may also help bring the absorbance back to the measurable range of the spectrometer. Weak absorption features (e.g., small sample size, inefficient chromophore) can be enhanced by extending the light path and prolonging the measurement time (i.e., increasing the exposure time or averaging the intensities from multiple measurements).

The ideal light source for a UV-Vis-NIR spectrometer provides white light with a homogeneous intensity across the entire spectrum range, though no single light source fits this criterion yet. LED lights with discontinuous spectra or fluorescent lights with sharp emission peaks are generally not suitable for a UV-Vis-NIR spectrometer. Instead, a tungsten-halogen lamp with a broad emission band spread across 350–1000 nm is typically used to cover the Vis-NIR range, and a deuterium lamp or xenon arc lamp can be used to cover the UV range between 200 and 400 nm. These lamps may operate separately to prolong their lifetime, depending on the range being measured, or together to cover the entire UV-Vis-NIR range. Multiple detector or monochromator types are sometimes used in scanning spectrophotometers to compensate for reduced efficiency or accuracy in different ranges. Switching between these components may introduce step-shaped artifacts in the measured spectrum, though their positions can often be adjusted to avoid significant interference with real features in the data.

dominantly colored by copper (Paraíba tourmaline) and tourmaline colored mainly by iron. Although vividly bright neon blue or green Paraíba tourmaline can often be identified visually, the color of some samples with lower saturation and tone may overlap with tourmaline dominantly colored by iron. UV-Vis-NIR spectroscopy provides a clear distinction: Cu^{2+} in tourmaline has two absorption bands at about 697 and 900 nm (Fritsch et al., 1990; Shigley et al., 2001), while Fe^{2+} has only a single band at about 715 nm (figure 2) within the measured range. Although some tourmalines have comparable color

Figure 2. Absorption spectra of copper-dominant Paraíba tourmaline (left) and iron-dominant tourmaline (right).

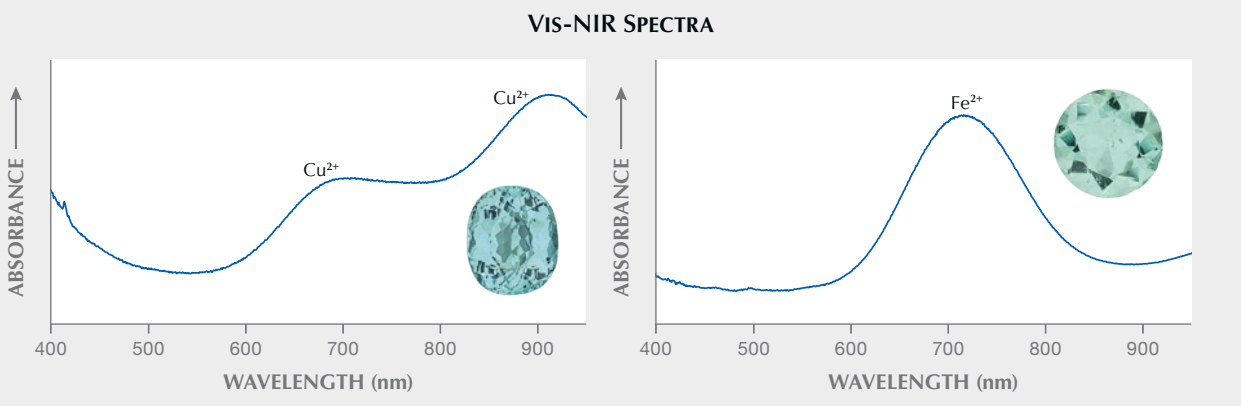

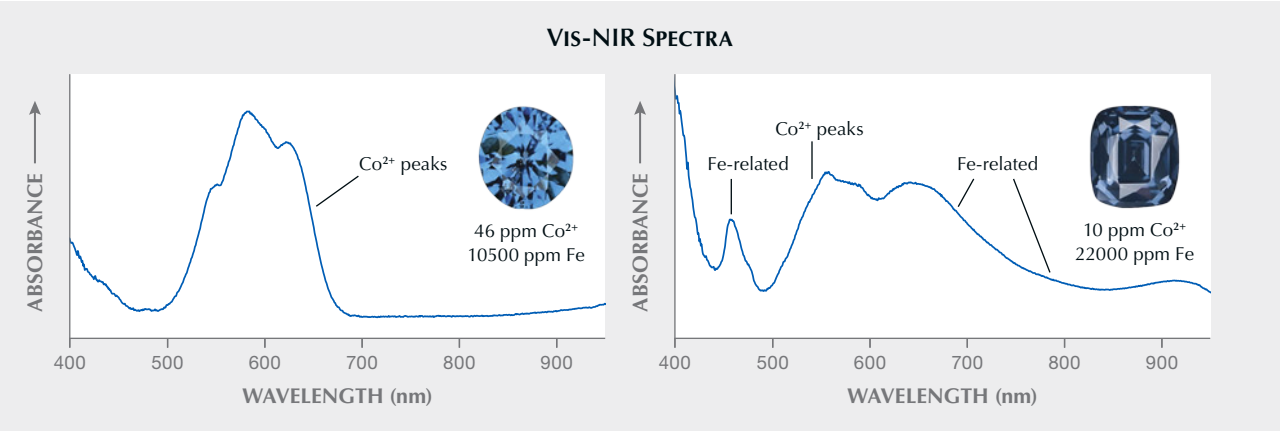

Figure 3. Example absorption spectra of a cobalt spinel (left) and a grayish blue spinel that does not meet the criteria due to its color and the significant influence of iron on its color (right).

contributions from both Cu^{2+} and Fe^{2+}, the end members can be easily separated. Those intermediate stones are a subject of further research that is outside the scope of this article.

Blue Spinel. Another common application of UV-Vis-NIR spectroscopy is distinguishing between blue spinel dominantly colored by cobalt and spinel with a significant iron component. Co^{2+} has a unique spectral pattern, with several peaks from 540 to 622 nm (figure 3, left) (D'Ippolito et al., 2015; Palke and Sun, 2018). Iron also has several possible absorption features in the visible range, including narrow bands at 459 and 473 nm likely related to Fe^{3+}, as well as broad bands around 650 and 900 nm and relatively sharp bands around 555 nm that overlap with Co^{2+} absorption features (figure 3, right). It is important to note that blue color in spinel is caused exclusively by Co^{2+}, while iron-related absorption alters the color by adding gray, purple, or greenish components. Determining whether a blue spinel qualifies as "cobalt spinel" requires a multivariate approach that considers its color, chemistry, and UV-Vis-NIR absorption spectrum together.

Aquamarine vs. Maxixe Beryl. UV-Vis-NIR can also be used to distinguish aquamarine from Maxixe beryl. Aquamarine's blue color is caused by the presence of Fe^{2+}, whose absorption can be intensified by the presence of Fe^{3+} (Taran and Rossman, 2001). Maxixe beryl derives its blue color from radiation. Figure 4 (left) shows a typical aquamarine spectrum, featuring a dominant absorption feature at about 830 nm producing the blue color. This absorption feature is also highly polarizable, with the maximum intensity perpendicular to the *c*-axis (the long dimension of most

Figure 4. Absorption spectra of aquamarine (left) and Maxixe beryl (right).

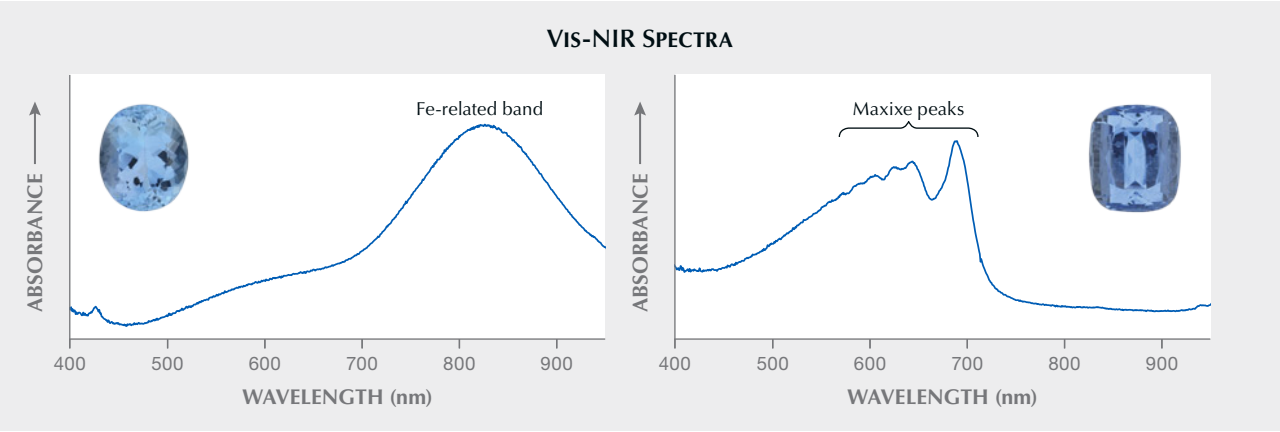

aquamarine crystals). As a result, an aquamarine's blue color appears most intense when the crystal is viewed perpendicular to the *c*-axis; it displays almost no color when viewed along the *c*-axis. In contrast, Maxixe beryl's pleochroic colors are the opposite, with the most intense blue color displayed down the *c*-axis and a weaker blue color perpendicular to the *c*-axis. The distinct UV-Vis-NIR spectrum of Maxixe beryl can also aid in its identification (Adamo et al., 2008). Maxixe beryl has a prominent, fairly narrow peak at about 691 nm, with several smaller peaks at shorter wavelengths of about 646, 630, 607, and 590 nm. These features typically overlay a relatively broad absorption band centered at roughly 620 nm (figure 4, right). It is important to be able to distinguish Maxixe beryl, as its radiation-induced blue color is often unstable and may fade with time.

Magmatic vs. Metamorphic Sapphire. Geographic origin determination for blue sapphire can be an extremely complicated and difficult task. Determining the geological origin of a sapphire, whether metamorphic or magmatic, can be simplified by reducing the number of origins to consider. The UV-Vis-NIR spectrum for sapphires of magmatic origin (e.g., Australia, Thailand, Cambodia, Nigeria, and Ethiopia) shows a pronounced absorption feature at 880 nm. Sapphires of metamorphic origin (e.g., Sri Lanka, Myanmar, Madagascar, and Kashmir) either lack this feature or show an 880 nm band of lower intensity than the Fe^{2+}-Ti^{4+} IVCT band at 580 nm (figure 5) (Palke et al., 2019). The origin of the 880 nm band is unclear but may be related to some combination of iron and titanium ions in corundum (Fritsch and Rossman, 1988; Moon and Phillips, 1994; Hughes et al., 2017). "Nonclassical" sapphire from Tanzania and Montana will show a UV-Vis-NIR spectrum more similar to metamorphic sapphire, lacking the 880 nm feature, but show pronounced Fe^{3+} absorption bands at 378, 388, and 450 nm (Dubinsky et al., 2020). One complication is that some higher-iron metamorphic sapphires may take on a magmatic-looking absorption pattern after low-temperature heating (Hughes and Perkins, 2019).

Jadeite (Natural vs. Dyed Color). The color origin of jadeite (natural or dyed) can also be determined by UV-Vis-NIR spectroscopy. A common cause of green color in jadeite is from Cr^{3+} with broad absorption bands around 454 and 645 nm and a sharp feature around 691 nm (figure 6A). While these can often be observed with a handheld spectroscope, a UV-Vis-NIR spectrometer can be helpful in cases where a jadeite is mounted or it is difficult to transmit light through the piece and into the spectroscope. Fe^{2+} can also cause green color in jadeite, though this green color is never as vibrant and vivid as that in high-quality chromium-colored jadeite. Fe^{2+} bands in jadeite can be seen at around 769 and 940 nm (figure 6B). Fe^{3+} absorption features may also be seen as sharp

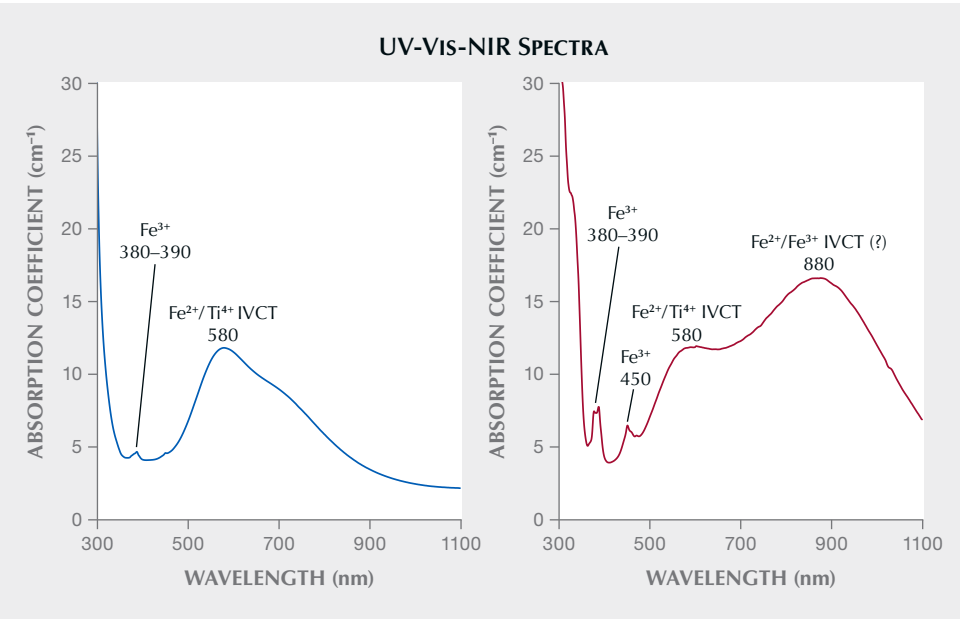

Figure 5. Absorption spectra showing the different intensities of the 880 nm band between metamorphic sapphire (left) and magmatic sapphire (right). From Palke et al. (2019).

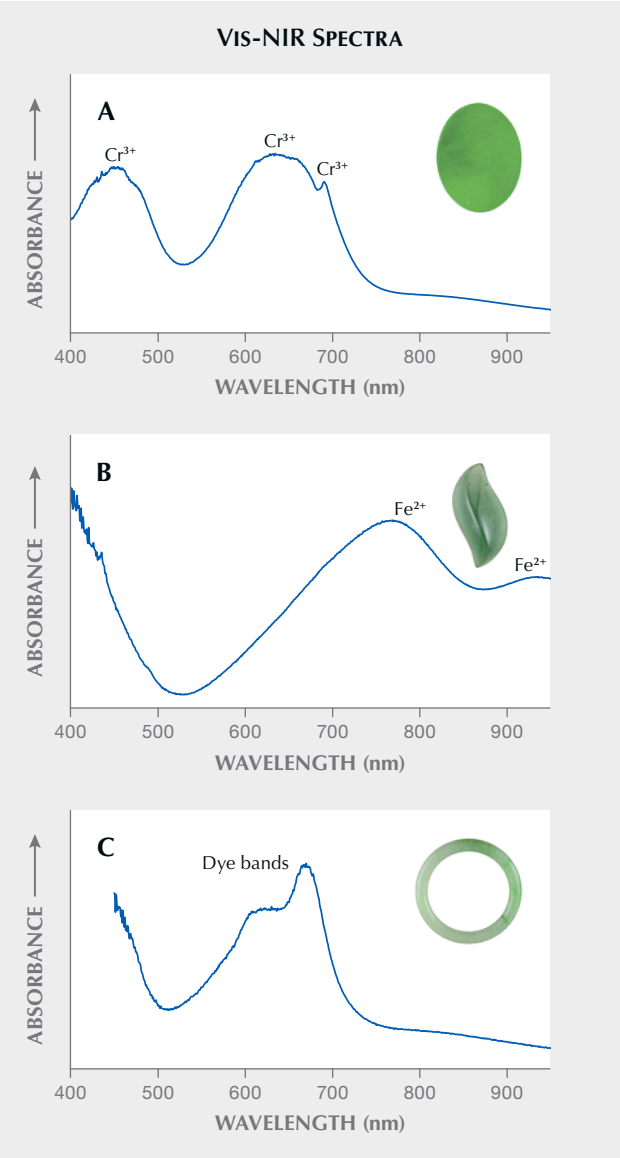

Figure 6. Examples of Vis-NIR spectra of jadeite colored by Cr^{3+} (A), Fe^{2+} (B), and artificial dyes (C).

bands at about 369, 381, 431, and 473 nm, but their effect on color is usually minimal. Dyed green jadeite has an entirely different absorption spectrum, typically displaying a double peak at around 620 and 669 nm (figure 6C). Similar criteria can also be used to separate dyed from natural-color lavender jadeite (Lu, 2012).

Chrome Varieties (Garnet, Tourmaline, Diopside, and Chalcedony). To be considered chrome varieties, the color of garnet, tourmaline, diopside, and chalcedony must be predominantly derived from the presence of chromium (and/or vanadium in the case of some tourmaline and diopside). The presence of chromium is easily confirmed in a UV-Vis-NIR spectrum by the presence of the characteristic Cr^{3+} absorption pattern consisting of two broad peaks. Figure 7 compares two green tourmalines, one colored by Cr^{3+} and the other by Fe^{2+}. Similar absorption patterns have been observed for other chromium-colored gems. Note that V^{3+} often shows an absorption pattern very similar to that of Cr^{3+} for green gems such as emerald or tourmaline, and the so-called chrome variety in the gem trade often includes certain green gemstones predominantly colored by vanadium.

Fancy-Color Diamonds. Because colorless diamonds typically do not show any useful features in the UV-Vis-NIR range, optical spectroscopy is used primarily for testing diamonds with fancy colors. Whereas the colors of colored gemstones can be predicted quite accurately just from their chemical compositions, the light-absorbing features of diamond depend on the exact configurations of defects and defect clusters. Despite the simple chemistry of diamond, it has numerous types of light-absorbing defects and defect clusters, many of which are still poorly understood. Color-causing defects in diamond could easily constitute a set of review articles or even monographs (Zaitsev, 2001; Dischler, 2012; Green et al., 2022). Only a few representative examples will be presented here to showcase the complexity of diamond identification and how it can be facilitated by UV-Vis-NIR spectroscopy.

UV-Vis-NIR spectra of diamonds are typically collected at liquid nitrogen temperatures, as the characteristic sharp absorption features of several defects are temperature sensitive. But the room-temperature spectrum also provides valuable information about the impact of different color centers on the diamond's overall bodycolor. Therefore, the handheld spectroscope can be used to observe many of the spectral features of a diamond, particularly one with strong color.

During crystallization, elements such as nitrogen, boron, and hydrogen can be incorporated into the diamond structure. Annealing at high-pressure, high-temperature (HPHT) conditions, as well as radiation after crystallization, can create new defects, destroy existing ones, or modify them into different configurations. Therefore, identifying the defect types in a diamond helps reveal its temperature, pressure, and radiation history. The different conditions required for each defect to form can potentially distinguish natural colors from colors created by treatment

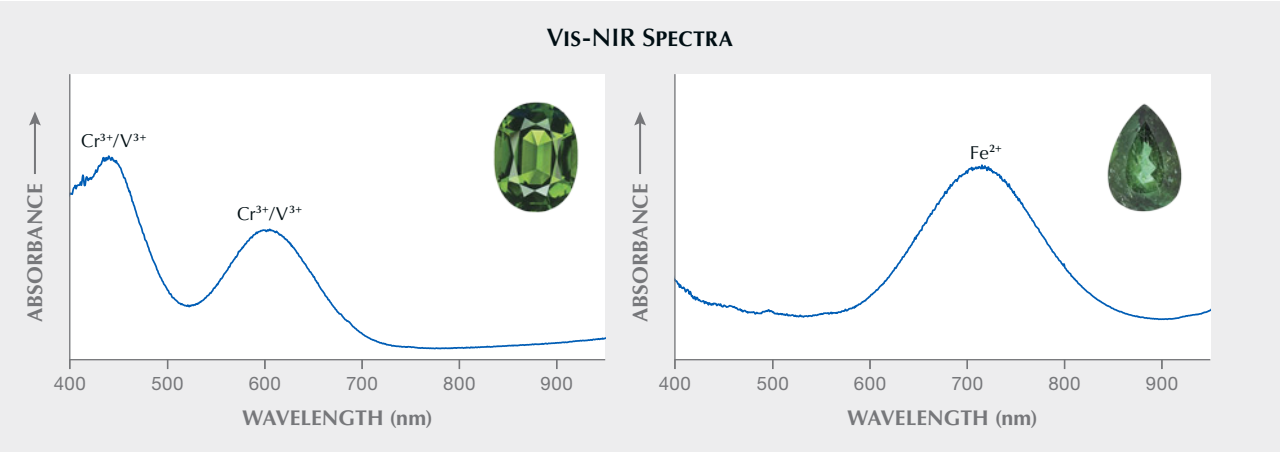

Figure 7. Absorption spectra of chrome tourmaline (left) and iron-colored green tourmaline (right).

processes. Some defects or combinations of defects in diamonds can only form naturally, requiring the extreme temperature-pressure conditions only found deep in the earth, while others require geological timescales for the defects to cluster into certain configurations. These defects may or may not survive certain treatment processes. Some defects are only found in laboratory-grown or treated diamonds, as the conditions needed to create them rarely occur or do not exist in nature. Of course, some defects can be created both naturally and artificially, particularly when the natural conditions responsible are easily replicated in a laboratory.

Fancy Yellow Diamond. Yellow is one of the most common colors in diamond. In fact, many light-colored diamonds are treated to intensify their colors beyond the D-to-Z color scale so they can be graded as fancy-color diamonds with potentially higher value. This yellow hue can be attributed to several types of defects. Four common types are isolated nitrogen defects (C center), the H3 (N_2V^0) defect, the "cape" series defect, and the 480 nm band defect (Breeding et al., 2020).

Isolated nitrogen produces a broad absorption band that peaks in the UV range and extends into the blue region (figure 8). Though all nitrogen-bearing diamonds can contain C centers, those with most nitrogen atoms in isolation, known as type Ib diamonds, are rare in nature, making up only 0.1% of all natural diamonds (Breeding et al., 2020). However, C centers are responsible for the color of most laboratory-grown yellow diamonds. The H3 (N_2V^0) defect consists of two nitrogen atoms surrounding a

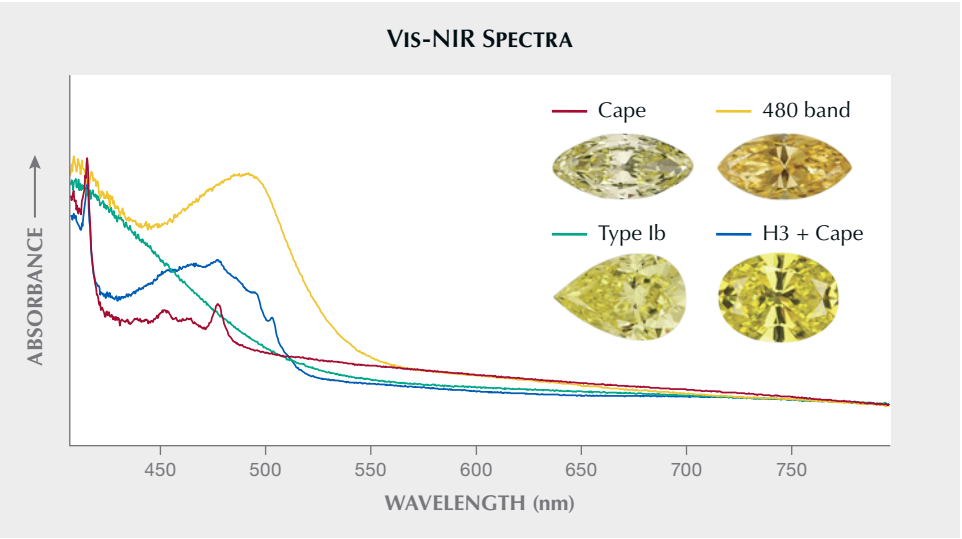

Figure 8. A comparison of four yellow diamonds colored by different defects. The absorption spectra were collected at liquid nitrogen temperature using the configuration shown in figure A-1D. The cape diamond and the 480 band diamond are both natural, while the type Ib diamond is laboratory grown. The H3 + cape diamond was irradiated and annealed to enhance its yellow color.

neutral vacancy with broad absorption in the blue region, characterized by a sharp peak at 503.2 nm (again, see figure 8) (Breeding et al., 2020), which imparts a yellow bodycolor to a diamond. Both C centers and H3 (N_2V^0) defects can be introduced by HPHT treatment to enhance the yellow color. H3 (N_2V^0) defects can also be created by irradiation followed by annealing.

"Cape" series absorption features, named after their original association with South Africa, can occur in diamonds from nearly all deposits. These consist of a series of bands in the blue to UV region, with prominent peaks at 415, 451, and 478 nm (figure 8), mostly related to the N3 (N_3V^0) defect (three nitrogen atoms around a single vacancy) (Mainwood, 1994). Much of the light yellow color in D-to-Z diamonds is due to various concentrations of cape series defects (King et al., 2008).

The defect structure of the wide absorption band centered at 480 nm (figure 8) is unknown, although it has been shown to be related to nickel and nitrogen (Breeding et al., 2020). This band creates yellow to orange color in diamond. Both the cape series and the 480 band are only known to occur naturally and have not been introduced through HPHT treatment.

Other Fancy-Color Diamonds. In addition to yellow, diamonds come in all other colors, each with its own unique defects and UV-Vis-NIR spectra. For instance, blue color can be caused by boron substitution, isolated vacancies, or rarely hydrogen-related defects (Eaton-Magaña et al., 2018). Green color in diamonds is commonly caused by radiation-induced vacancies plus absorption from more complex defects or hydrogen-related defects, though several additional but rarer cases can also produce green color (Breeding et al., 2018). Therefore, UV-Vis-NIR is helpful in identifying the specific defects present (i.e., what "kind" of green diamond). In addition to color-causing defects, there are also defects that contribute little to the color but provide clues as to the radiation and/or annealing history of the stone, indicating possible treatments. UV-Vis-NIR alone is not diagnostic, however, and requires further testing and gemological observation to determine a diamond's color origin with certainty.

Pearls. UV-Vis-NIR reflectance spectroscopy (figure A-1E) can be used to identify biological pigments responsible for natural color in pearls. This helps differentiate between naturally and artificially colored pearls, especially when visual evidence is absent. The untreated colors of pearls, whether natural or cultured, are mainly caused by a mixture of biological pigments associated with the mollusk species producing the pearls. Different mollusk species create pearls in different color ranges. The major pigments across various species are porphyrin and polyenic groups (Iwahashi and Akamatsu, 1994; Karampelas et al., 2007), as well as melanin (Jabbour-Zahab et al., 1992; Wang et al., 2020). And in some cases, unidentified pigments were reported to be responsible for the yellow coloration of saltwater pearls produced from *Pinctada* species (Karampelas et al., 2020).

For pearls, reflection spectra are generally obtained in the 250–800 nm range. It should be noted that reflectance refers to the light not absorbed by the surface, which means a reflection spectrum is interpreted in the opposite way as an absorption spectrum. Absorption features that appear as peaks in an absorption spectrum will appear as dips in a reflection spectrum. The bodycolor of a pearl corresponds to the high-reflectance regions in the reflection spectrum that are less affected by absorption features. Almost all pearls show a common absorption feature at about 280 nm that is associated with conchiolin, a mixture of protein and polysaccharides found in pearls and shells. In the visible range, the spectra for white and very light-colored pearls are relatively featureless due to weak or absent pigmentation, while darker and more saturated pearls exhibit lower reflectance in their spectra and more prominent absorption features. Strong overtone or iridescence colors on the surface may impact the spectrum patterns.

Dark-Colored Nacreous Pearls. Dark, natural-color saltwater nacreous pearls, ranging from light gray, gray, and brown to black with various hues such as green and blue, display characteristic absorption features at 405 and/or 495 nm (Elen, 2002; Karampelas et al., 2011). These features can be used to separate them from artificial dark colors created by dye (figure 9). The 405 nm feature is reported to be from uroporphyrin pigmentation (Iwahashi and Akamatsu, 1994), while the 495 nm feature is possibly related to a type of porphyrin.

Most of the dark-colored pearls on the market are known as Tahitian pearls, produced from *Pinctada margaritifera*. These and the closely related pearls from *P. mazatlanica* display a diagnostic feature at 700 nm (Wada, 1984; Homkrajae, 2016) that can be used to separate them from other natural dark-colored pearls, including other *Pinctada* species (Karampelas, 2012; Homkrajae, 2016; Nilpetploy et al., 2018; Al-

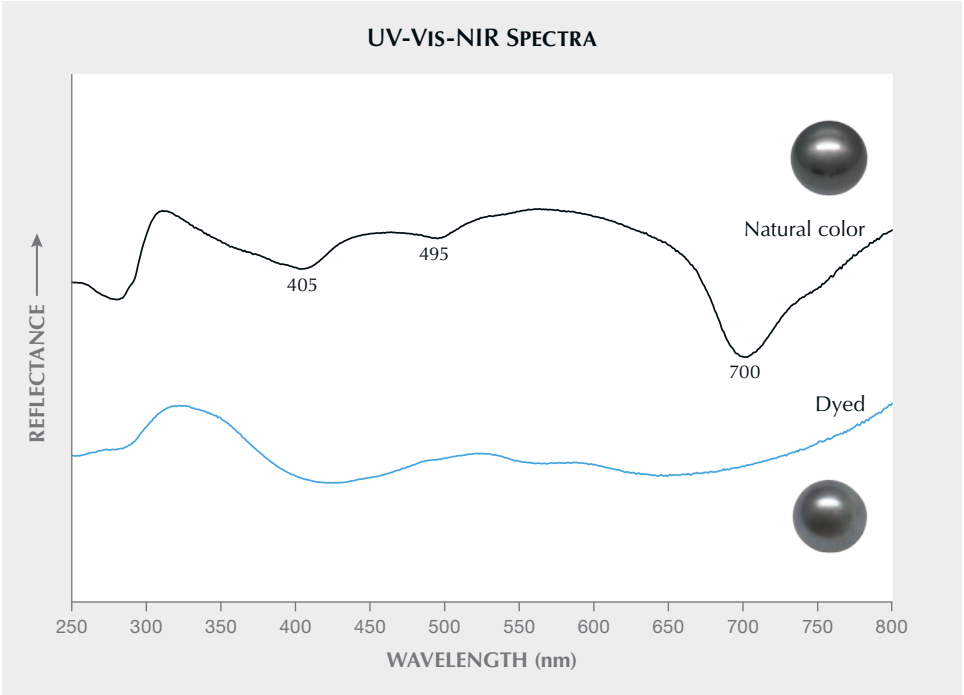

Figure 9. Reflectance spectra of dark gray nacreous pearls, natural and dyed. A natural-color Tahitian pearl exhibits characteristic absorption features at 405 and 495 nm, together with a diagnostic 700 nm feature of the P. margaritifera *mollusk. The natural pigmentation features are absent in the spectra of dyed dark gray pearls.*

Alawi et al., 2020), *Pteria* pearls (Kiefert et al., 2004), and windowpane oyster pearls produced by the Placunidae family (Ho et al., 2024).

Additionally, a series of chemical and physical processes has been reported to lighten naturally gray to dark gray Tahitian pearls to "chocolate" and "pistachio" colors. Since this color alteration is achieved by modifying or removing certain natural pigments, no foreign coloring agent can be detected on the surface. UV-Vis-NIR reflectance spectra obtained from the treated "chocolate" and "pistachio" pearls still show the natural pigment features, but they become

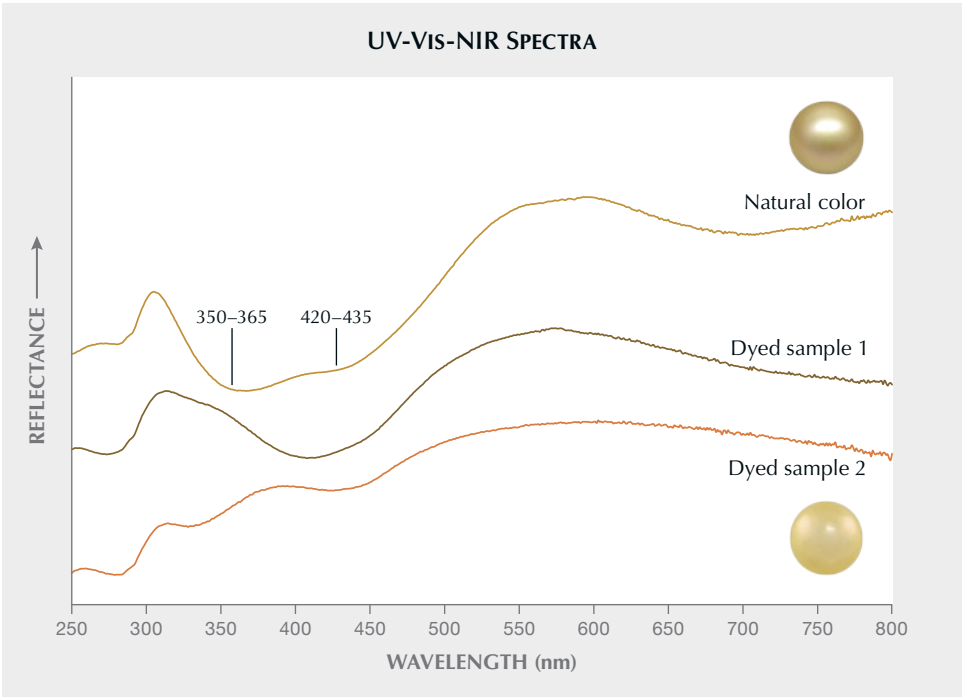

Figure 10. Reflectance spectra of natural and treated yellow nacreous pearls. A natural-color South Sea pearl exhibits a broad absorption region between 330 and 460 nm, consisting of two distinct bands at 350–365 nm and 420–435 nm. Dyed yellow pearls normally have an absence of this characteristic or the presence of different absorption features in the blue region of the spectrum.

broader and the centers are shifted from the 405 and 495 nm positions (Wang et al., 2006; Zhou et al., 2016). The diagnostic 700 nm feature for *P. margaritifera* (Tahitian) remains unchanged in these treated pearls.

Yellow Nacreous Pearls. Yellow colors in pearls are caused by preferential absorbance of light in the long-wave UV to blue region of the spectrum, with most of the green to red light reflected by the surface. Yellow and orangy yellow *Pinctada maxima* pearls, commonly known as golden South Sea pearls, are among the most desirable pearls in the market. Natural-color yellow South Sea pearls typically show a broad absorption region between 330 and 460 nm (figure 10). This broad region usually consists of two absorption features, the first centered between 350 and 365 nm and the second between 420 and 435 nm (Elen, 2001). Similar absorption features have also been observed in yellow-hued pearls produced by other species, including *P. margaritifera* (Karampelas et al., 2011), *P. mazatlanica* (Homkrajae, 2016), and *P. maculata* (Nilpetploy et al., 2018). The absence of this characteristic or the presence of different absorption features in the blue region of the spectrum indicates an unnatural origin for the yellow color (figure 10) (Elen, 2001, 2002; Zhou et al., 2012).

Heat treatment has been reported to create uniform and enhanced colors in cream and light yellow pearls. This process supposedly does not introduce any external dye materials into the pearl. Therefore, the characteristic absorption features observed in natural-color pearls appear much weaker or completely absent in heated yellow pearls with the same color (Elen, 2001; Zhou et al., 2012).

The natural colors in freshwater pearls are caused by a mixture of various polyenic pigments (Karampelas et al., 2009, 2020), which display absorption features in the range of violet to yellow (405–568 nm) of the visible spectrum (Karampelas et al., 2009; Homkrajae et al., 2019). Unfortunately, these features in freshwater pearls are much more complicated and difficult to identify than those in saltwater pearls and thereby not useful for identification purposes. Raman spectroscopy is more useful for identifying the polyenic pigments in freshwater pearls (Jin and Smith, 2024).

CONCLUSIONS

At first glance, the UV-Vis-NIR spectrometer might seem the simplest analytical testing instrument in a gemological laboratory, as it employs the same basic principles as a handheld spectroscope. However, its application to gemology is one of the most far-reaching across all categories of gemstones, since color is such a significant value factor for colored stones, fancy-color diamonds, and pearls. Due to the wide range of size, shape, form, and diaphaneity of gemstones, measuring their UV-Vis-NIR spectra is often challenging. Specialized instruments and configurations have been designed for specific applications, such as mounted jewelry, opaque materials, and even liquid nitrogen measurements, all of which require special procedures for testing. Unlike Raman spectroscopy, which can be automated by computer programs to a great extent, interpreting a UV-Vis-NIR spectrum is not nearly as straightforward. Rigorous training and extensive practice are required for a gemologist to separate the true signals from noise and instrument artifacts and make a correct assessment. As demonstrated by the examples presented in this article, considerable information is hidden behind the striking colors of gemstones. In fact, the mechanisms of many colors in gemstones are still not fully understood. For instance, the exact electronic transition and defect configuration of amethyst, blue zircon, and many light-absorbing features in diamonds are still unknown. The light-absorbing defects in gem materials, as well as their reactions to treatments, are the subject of a very active research field in gemology, and new discoveries constantly emerge. As our understanding of the causes of colors in gems deepens, the utility of UV-Vis-NIR spectroscopy continues to grow.

ABOUT THE AUTHORS

Dr. Shiyun Jin is a research scientist, Nathan Renfro is senior manager of colored stone identification, Dr. Aaron Palke is senior manager of research, Troy Ardon is a senior research engineer, and Artitaya Homkrajae is supervisor of pearl identification at GIA in Carlsbad, California.

ACKNOWLEDGMENTS

The authors thank the peer reviewers for many constructive comments and suggestions.

REFERENCES

Adamo I., Pavese A., Prosperi L., Diella V., Ajò D., Gatta G.D., Smith C.P. (2008) Aquamarine, Maxixe-type beryl, and hydrothermal synthetic blue beryl: Analysis and identification. *G&G*, Vol. 44, No. 3, pp. 214–226, http://dx.doi.org/10.5741/GEMS.44.3.214

Al-Alawi A., Ali Z., Rajab Z., Albedal F., Karampelas S. (2020) Saltwater cultured pearls from *Pinctada radiata* in Abu Dhabi (United Arab Emirates). *Journal of Gemmology*, Vol. 37, No. 2, pp. 164–179.

Anderson B.W., Payne C.J., Mitchell R.K. (1998) *The Spectroscope and Gemmology*. GemStone Press, Woodstock, Vermont.

Baier E. (1932) Die optik der edelopale. *Zeitschrift für Kristallographie - Crystalline Materials*, Vol. 81, No. 1-6, pp. 183–218, http://dx.doi.org/10.1524/zkri.1932.81.1.183

Bolton H.C., Bursill L.A., McLaren A.C., Turner R.G. (1966) On the origin of the colour of labradorite. *Physica Status Solidi (b)*, Vol. 18, No. 1, pp. 221–230, http://dx.doi.org/10.1002/pssb.19660180123

Breeding C.M., Ahline N. (2024) Infrared spectroscopy and its use in gemology. *G&G*, Vol. 60, No. 4, pp. 474–492, http://dx.doi.org/10.5741/GEMS.60.4.474

Breeding C.M., Shen A.H., Eaton-Magaña S., Rossman G.R., Shigley J.E., Gilbertson A. (2010) Developments in gemstone analysis techniques and instrumentation during the 2000s. *G&G*, Vol. 46, No. 3, pp. 241–257, http://dx.doi.org/10.5741/GEMS.46.3.241

Breeding C.M., Eaton-Magaña S., Shigley J.E. (2018) Natural-color green diamonds: A beautiful conundrum. *G&G*, Vol. 54, No. 1, pp. 2–27, http://dx.doi.org/10.5741/GEMS.54.1.2

——— (2020) Naturally colored yellow and orange gem diamonds: The nitrogen factor. *G&G*, Vol. 56, No. 2, pp. 194–219, http://dx.doi.org/10.5741/GEMS.56.2.194

D'Ippolito V., Andreozzi G.B., Hålenius U., Skogby H., Hametner K., Günther D. (2015) Color mechanisms in spinel: Cobalt and iron interplay for the blue color. *Physics and Chemistry of Minerals*, Vol. 42, No. 6, pp. 431–439, http://dx.doi.org/10.1007/s00269-015-0734-0

Dischler B. (2012) *Handbook of Spectral Lines in Diamond*. Springer, Berlin, Heidelberg.

Dowty E. (1978) Absorption optics of low-symmetry crystals—Application to titanian clinopyroxene spectra. *Physics and Chemistry of Minerals*, Vol. 3, No. 2, pp. 173–181, http://dx.doi.org/10.1007/BF00308120

Dubinsky E.V., Stone-Sundberg J., Emmett J.L. (2020) A quantitative description of the causes of color in corundum. *G&G*, Vol. 56, No. 1, pp. 2–28, http://dx.doi.org/10.5741/GEMS.56.1.2

Eaton-Magaña S., Breeding C.M., Shigley J.E. (2018) Natural-color blue, gray, and violet diamonds: Allure of the deep. *G&G*, Vol. 54, No. 2, pp. 112–131, http://dx.doi.org/10.5741/GEMS.54.2.112

Elen S. (2001) Spectral reflectance and fluorescence characteristics of natural-color and heat-treated "golden" South Sea cultured pearls. *G&G*, Vol. 37, No. 2, pp. 114–123, http://dx.doi.org/10.5741/GEMS.37.2.114

——— (2002) Identification of yellow cultured pearls from the black-lipped oyster *Pinctada margaritifera*. *G&G*, Vol. 38, No. 1, pp. 66–72, http://dx.doi.org/10.5741/GEMS.38.1.66

Emmett J.L., Douthit T.R. (1993) Heat treating the sapphires of Rock Creek, Montana. *G&G*, Vol. 29, No. 4, pp. 250–272, http://dx.doi.org/10.5741/GEMS.29.4.250

Fritsch E., Rossman G.R. (1988) An update on color in gems. Part 2: Colors involving multiple atoms and color centers. *G&G*, Vol. 24, No. 1, pp. 3–15, http://dx.doi.org/10.5741/GEMS.24.1.3

Fritsch E., Shigley J.E., Rossman G.R., Mercer M.E., Muhlmeister S.M., Moon M. (1990) Gem-quality cuprian-elbaite tourmalines from São José Da Batalha, Paraíba, Brazil. *G&G*, Vol. 26, No. 3, pp. 189–205, http://dx.doi.org/10.5741/GEMS.26.3.189

Green B.L., Collins A.T., Breeding C.M. (2022) Diamond spectroscopy, defect centers, color, and treatments. *Reviews in Mineralogy and Geochemistry*, Vol. 88, No. 1, pp. 637–688, http://dx.doi.org/10.2138/rmg.2022.88.12

Heaney P.J. (2021) Iris agates and cantor dusts: The textural complexity of agates. In *Seventeenth Annual Sinkankas Symposium—Agate and Chalcedony*. Pala International, Inc., pp. 29–39.

Ho J.W.Y., Lawanwong K., Homkrajae A. (2024) Lab Notes: Pearls from the Placunidae family (windowpane oysters). *G&G*, Vol. 60, No. 1, pp. 69–71.

Homkrajae A. (2016) Gem News International: Spectral characteristics of *Pinctada mazatlanica* and *Pinctada margaritifera* pearl oyster species. *G&G*, Vol. 52, No. 2, pp. 207–208.

Homkrajae A., Sun Z., Shih S.C. (2019) Gem News International: Gemological and chemical characteristics of natural freshwater pearls from the Mississippi River system. *G&G*, Vol. 55, No. 2, pp. 280–285.

Hughes E.B., Perkins R. (2019) Madagascar sapphire: Low-temperature heat treatment experiments. *G&G*, Vol. 55, No. 2, pp. 184–197, http://dx.doi.org/10.5741/GEMS.55.2.184

Hughes R.W., Manorotkul W., Hughes E.B. (2017) *Ruby & Sapphire: A Gemologist's Guide*. RWH Publishing, Bangkok.

Iwahashi Y., Akamatsu S. (1994) Porphyrin pigment in black-lip pearls and its application to pearl identification. *Fisheries Science*, Vol. 60, No. 1, pp. 69–71, http://dx.doi.org/10.2331/fishsci.60.69

Jabbour-Zahab R., Chagot D., Blanc F., Grizel H. (1992) Mantle histology, histochemistry and ultrastructure of the pearl oyster *Pinctada margaritifera* (L.). *Aquatic Living Resources*, Vol. 5, No. 4, pp. 287–298, http://dx.doi.org/10.1051/alr:1992027

Jin S., Smith E.M. (2024) Raman spectroscopy and X-ray diffraction in gemology: Identifying mineral species and other phases. *G&G*, Vol. 60, No. 4, pp. 518–535, http://dx.doi.org/10.5741/GEMS.60.4.518

Jin S., Sun Z., Palke A.C. (2022) Color effects of Cu nanoparticles in Cu-bearing plagioclase feldspars. *American Mineralogist*, Vol. 107, No. 12, pp. 2188–2200, http://dx.doi.org/10.2138/am-2022-8325

Jin S., Palke A.C., Renfro N.D., Sun Z. (2023) Special colors and optical effects of Oregon sunstone: Absorption, scattering, pleochroism, and color zoning. *G&G*, Vol. 59, No. 3, pp. 298–322, http://dx.doi.org/10.5741/GEMS.59.3.298

Jollands M., Ludlam A., Palke A.C., Vertriest W., Jin S., Cevallos P., Arden S., Myagkaya E., D'Haenens-Johannson U., Weeramongkhonlert V., Sun Z. (2023) Color modification of spinel by nickel diffusion: A new treatment. *G&G*, Vol. 59, No. 2, pp. 164–181, http://dx.doi.org/10.5741/GEMS.59.2.164

Karampelas S. (2012) Spectral characteristics of natural-color saltwater cultured pearls from *Pinctada maxima*. *G&G*, Vol. 48, No. 3, pp. 193–197, http://dx.doi.org/10.5741/GEMS.48.3.193

Karampelas S., Fritsch E., Mevellec J.-Y., Gauthier J.-P., Sklavounos S., Soldatos T. (2007) Determination by Raman scattering of the nature of pigments in cultured freshwater pearls from the mollusk *Hyriopsis cumingi*. *Journal of Raman Spectroscopy*, Vol. 38, No. 2, pp. 217–230, http://dx.doi.org/10.1002/jrs.1626

Karampelas S., Fritsch E., Mevellec J.-Y.S., Soldatos T. (2009) Role of polyenes in the coloration of cultured freshwater pearls. *European Journal of Mineralogy*, Vol. 21, No. 1, pp. 85–97, http://dx.doi.org/10.1127/0935-1221/2009/0021-1897

Karampelas S., Fritsch E., Gauthier J.-P., Hainschwang T. (2011) UV-Vis-NIR reflectance spectroscopy of natural-color saltwater cultured pearls from *Pinctada margaritifera*. *G&G*, Vol. 47, No. 1, pp. 31–35, http://dx.doi.org/10.5741/GEMS.47.1.31

Karampelas S., Fritsch E., Makhlooq F., Mohamed F., Al-Alawi A. (2020) Raman spectroscopy of natural and cultured pearls and pearl producing mollusc shells. *Journal of Raman Spectroscopy*, Vol. 51, No. 9, pp. 1813–1821, http://dx.doi.org/10.1002/jrs.5670

Kiefert L., Moreno D.M., Arizmendi E., Hänni H.A., Elen S. (2004)

Cultured pearls from the Gulf of California, Mexico. *G&G*, Vol. 40, No. 1, pp. 26–38, http://dx.doi.org/10.5741/GEMS.40.1.26
King J.M., Geurts R.H., Gilbertson A.M., Shigley J.E. (2008) Color grading "D-to-Z" diamonds at the GIA Laboratory. *G&G*, Vol. 44, No. 4, pp. 296–321, http://dx.doi.org/10.5741/GEMS.44.4.296
Kitawaki H., Abduriyim A., Okano M. (2006) Identification of heat-treated corundum. *G&G*, Vol. 42, No. 3, p. 84.
Koivula J.I., Kammerling R.C. (1989) Gem News: New developments in spectroscopy. *G&G*, Vol. 25, No. 1, pp. 49–50.
Lu R. (2012) Color origin of lavender jadeite: An alternative approach. *G&G*, Vol. 48, No. 4, pp. 273–283, http://dx.doi.org/10.5741/GEMS.48.4.273
Mainwood A. (1994) Nitrogen and nitrogen-vacancy complexes and their formation in diamond. *Physical Review B*, Vol. 49, No. 12, pp. 7934–7940, http://dx.doi.org/10.1103/PhysRevB.49.7934
Moon A.R., Phillips M.R. (1994) Defect clustering and color in Fe,Ti: α-Al_2O_3. *Journal of the American Ceramic Society*, Vol. 77, No. 2, pp. 356–367, http://dx.doi.org/10.1111/j.1151-2916.1994.tb07003.x
Moses T.M., Shigley J.E. (2003) G. Robert Crowningshield: A legendary gemologist. *G&G*, Vol. 39, No. 3, pp. 184–199, http://dx.doi.org/10.5741/GEMS.39.3.184
Nilpetploy N., Lawanwong K., Kessrapong P. (2018) The gemological characteristics of Pipi pearls reportedly from *Pinctada maculata*. *G&G*, Vol. 54, No. 4, pp. 418–427, http://dx.doi.org/10.5741/GEMS.54.4.418
Palke A.C., Sun Z. (2018) What is cobalt spinel? Unraveling the causes of color in blue spinels. *G&G*, Vol. 54, No. 3, p. 262.
Palke A.C., Saeseaw S., Renfro N.D., Sun Z., McClure S.F. (2019) Geographic origin determination of blue sapphire. *G&G*, Vol. 55, No. 4, pp. 536–579, http://dx.doi.org/10.5741/GEMS.55.4.536
Rossman G.R. (2014) Optical spectroscopy. *Reviews in Mineralogy and Geochemistry*, Vol. 78, No. 1, pp. 371–398, http://dx.doi.org/10.2138/rmg.2014.78.9
Shigley J.E., Cook B.C., Laurs B.M., Bernardes M.D.O. (2001) An update on "Paraíba" tourmaline from Brazil. *G&G*, Vol. 37, No. 4, pp. 260–276, http://dx.doi.org/10.5741/GEMS.37.4.260
Sun Z., Jollands M., Palke A. (2024) Chemical analysis in the gemological laboratory: XRF and LA-ICP-MS. *G&G*, Vol. 60, No. 4, pp. 536–559, http://dx.doi.org/10.5741/ GEMS.60.4.536
Taran M.N., Rossman G.R. (2001) Optical spectroscopic study of tuhualite and a re-examination of the beryl, cordierite, and osumilite spectra. *American Mineralogist*, Vol. 86, No. 9, pp. 973–980, http://dx.doi.org/10.2138/am-2001-8-903
Wada K. (1984) Spectral characteristics of pearls. *Hōseki gakkaishi*, Vol. 10, No. 4, pp. 95–103.
Wang W., Scarratt K., Hyatt A., Shen A.H.-T., Hall M. (2006) Identification of "chocolate pearls" treated by Ballerina Pearl Co. *G&G*, Vol. 42, No. 4, pp. 222–235, http://dx.doi.org/10.5741/GEMS.42.4.222
Wang Z., Adzigbli L., Zheng Z., Yang C., Deng Y. (2020) How cultured pearls acquire their colour. *Aquaculture Research*, Vol. 51, No. 10, pp. 3925–3934, http://dx.doi.org/10.1111/are.14765
Zaitsev A.M. (2001) *Optical Properties of Diamond*. Springer, Berlin, Heidelberg.
Zhou C., Homkrajae A., Ho J.W.Y., Hyatt A., Sturman N. (2012) Update on the identification of dye treatment in yellow or "golden" cultured pearls. *G&G*, Vol. 48, No. 4, pp. 284–291, http://dx.doi.org/10.5741/GEMS.48.4.284
Zhou C., Ho J.W.Y., Chan S., Zhou J.Y., Wong S.D., Moe K.S. (2016) Identification of "pistachio" colored pearls treated by Ballerina Pearl Co. *G&G*, Vol. 52, No. 1, pp. 50–59, http://dx.doi.org/10.5741/GEMS.52.1.50

Thank You, Reviewers

GEMS & GEMOLOGY requires each manuscript submitted for publication to undergo a rigorous peer review process, in which each paper is evaluated by at least three experts in the field prior to acceptance. This is essential to the accuracy, integrity, and readability of *G&G* content. In addition to our dedicated Editorial Review Board, we extend many thanks to the following individuals who devoted their valuable time to reviewing manuscripts in 2024.

Non-Editorial Board Reviewers

Abeer Al-Alawi • Alessandra Altieri • Roy Bassoo • Philippe Belley • Thanh Nhan Bui • Athena Chen • Gagan Choudhary • James Conant • Emily Dubinsky • Elliot Entin • Alexander Falster • Hans Albert Gilg • Hertz Hasenfeld • Frank Hawthorne • Shiyun Jin • Michael Jollands • Yusuke Katsurada • Greg and Russell Kwiat • Jose Sasian • Travis Serio • Greg Stopka • Alexandre Zaitsev